Multiscale Characterization of Human Cortical Bone

Marie-Christine Ho Ba Tho, P.-E. Mazeran, K El Kirat, Sabine F Bensamoun

 CMES, vol.87, no.6, pp.557-577, 2012

Multiscale Characterization of Human Cortical Bone

MC. Ho Ba Tho[1], PE Mazeran[2], K El Kirat[1] and S.F. Bensamoun[1]

Abstract: Mechanical properties of cortical human bone have been investigated for more than four decades. Numerous experimental investigations on bone characterization were performed ; mechanical, vibrational, acoustical testing and morphological, physico-chemical investigations. Due to the techniques, different levels of investigation were performed and subsequently quantitative parameters are concerning different level of structure of bone (organ, tissue,...). According to our knowledge, few investigations were performed simultaneously on mechanical, morphological and physico-chemical properties of bone. The objectives of the present study were to investigate the influence of multiscale structural characteristics of the bone tissue on its mechanical behavior and to provide some estimations from micro-macro numerical modelling based on our experimental data.

Keywords: Mechanical properties, morphological properties, physico-chemical properties - human cortical bone.

1 Introduction

Mechanical properties of human bone have been assessed for more than four decades atdifferent levels of organisation (organ, tissue) deriving to a lot of data available in the literature. Experimental techniques assessing bone mechanical properties at the macro level werebased on wave propagation analysis and conventional mechanical testing (Ashman 1989). Preservation, size, type ofspecimen are of importance in the experimental design. An atlas of human cortical and cancellous bone has been performed (Ho Ba Tho et al. 1992, 1998) demonstrating the variation of the mechanical properties of bone according to the type, its anatomical location, and among subjects. Moreover the degree of anisotropy of human bone was investigated demonstrating an orthotropic mechanical behaviour for human short and long bones.

[1] Biomechanics and Bioengineering UTC, Compiègne, France.
[2] Roberval UTC, Compiègne, France.

At the microstructural level, acousticmicroscopy and micromechanical testing, allow the assessment of elastic properties of the osteon (Ascenzi et al. 1990, Meunier and Katz 1988, Ho Ba Tho and Laugier 2009). Recently nanoindentation techniques could provide better estimation of elastic properties of theosteon lamellae (Rho et al. 1997, 1999, Zysset et al. 1999). Anisotropic behavior determined experimentally or using micromechanics or finite element models, has been demonstrated by different authors (Fan et al. 2002, Fan et al. 2004, Hellmich et al. 2004, Carnelli et al. 2010). Viscoelastic behavior has been studied by Fan and Rho 2002 showing the time dependency of measurements on nanoindentation. Its viscoplastic behavior demonstrated the interaction between mineral and organic contents in bone (Vanleene et al. 2008, 2006). Another study suggests that the ultrastructural water may play a very important role as plastyfier (Fritsch et al. 2009). For the same tissue, different structural levels of investigation requiredifferent techniques.Numerous mathematical models exist at different levels from ultra-micromacro (Aoubiza et al. 1996, Hellmich et al. 2004, Crolet et al. 2005)micromacro (Katz 1981, Hogan 1992).Such studies are of importance for the assessment of the impactof bone pathologies and their treatments on skeletal functionality and on the understanding of themechanisms of cortical bone genesis.

In the present study, mechanical, morphological and physico-chemical characterization were studiedsimultaneously involving different scale levels from macromicro to ultra structural levels. These results will contribute to a basic understanding of the multiscale mechanical behavior of human cortical bone. In fact, the relationships between the mechanical behaviour of the bone at different scales will allow to get a better knowledge of the impact of the alterations of the mechanical properties from a scale to another scale.

2 Material and methods

2.1 Specimen of human cortical bone

Three human femurs (F1, F2, F3) were obtained from University Hospital of Amiens. These femurs exhibit different density reflecting significant alteration of structural properties. Themean values of their respective densities are 1892 ± 29 kg/m^3, 1608 ± 275 kg/m^3, 1221 ± 161 kg/m^3(figure 1). These values are corresponding the average densities measured macroscopically and physically (based on Archimedes principles and accurate balance) on samples obtained with these three femurs as mentioned below.

The femurswere sectionedtransversely with a low-speed diamond saw (MICRO-CUT2). Four sectionsbetween 40% and 70% of the total length of the femur were cut. The average thickness of the slices is 2.09 ± 0.27mmmeasured with a nu-

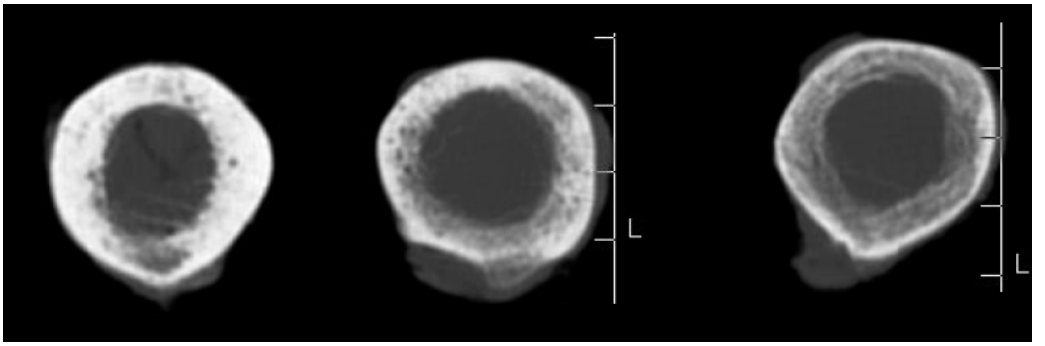

Figure 1: CT scans of the three femurs exhibiting different densities respectively from left to right F1, F2, F3.

merical device micrometer (Mitutoyo, 156-101, Mexico) which accuracyis 0.01 mm.Between the different slices, cubic and parallepiped cortical samples were obtained parallel to theaxis of the femur in the lateral, medial and posterior sides. A total of 60 samples was obtained (10 for F1 and 18 F3, and 32 for F2). Densities were measured with an accurate balance (August Sauter 424 Gmbh, Albstadt).

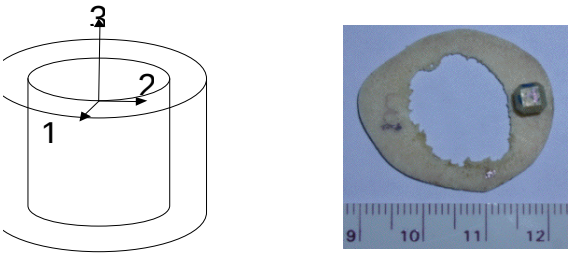

Figure 2: Cutting along the symmetry axes of the bone (3) longitudinal, (2) tangential, (1) radial axes.

2.2 Multi scale characterization

2.2.1 At the organ level (Macro structure).

At this level, it should specify that tissue properties are investigated across the organ at 100 μm resolution. Quantitative Computed Tomography (QCT) measurements and ultrasonic measurements were performed on the cross section specimens using the transmission ultrasonic technique by immersion (TUI) (Bensamoun et al. 2004). QCT measurements are largely used in order to investigate relationships

between mechanical properties and CT numbers (Rho et al. 1995), deriving to the development of individualized numerical modelling (Ho Ba Tho 2003). In the present study QCT protocol was performed before and after the cut of the cross section. The QCT protocol was optimised in order to assess density resolution (Ho Ba Tho et Treutenaere 2001). Calibration of CT numbers was performed with cortical bone with different densities measured experimentally using Archimedes principle. Then a cartography of densities could be provided. The TUItechnique consists in the measurements of longitudinal velocities which are determined through an ultrasonic method, whichoperates in transmission. The generator delivers electricalpulses. The pulses have been transmitted to thepiezoelectric transducer that transformed the electricsignal into an acoustic wave. Immersion transducer at 5MHz (Panametrics, V309, MA) with a focal length of75mm has been used. The diameter of the spot is1.24 mm.Both techniques allowed the spatial distribution of bulk velocities in the axial direction and the CT numbers. By registration and image fusion the spatial distribution of elastic constant C33 in the longitudinal direction could be then obtained (Figure 2).

2.2.2 At the tissue level (Macro-Micro structure)

At the tissue level, macro and micro measurements were performed using respectively two ultrasonic techniques immersion (TUI) and contact (TUC) and nanoindentation techniques. Anisotropy was also investigated at macro and micro structural levels.

Macrostructural level

The TUC technique allowed to measure the bar or bulk velocities according to the frequency of the transducers (Ho Ba Tho and Laugier 2009). An ultrasonic transmission technique developed in our laboratory allowed the anisotropic mechanical behaviour of the cortical bone to be assessed. In fact, bone was assumed to have an orthotropic behaviour which stiffness matrix is containing nine independent elastic constants. By reversing the stiffness matrix, the compliance matrix allowed the elastic properties in the three axes of symmetry of the crystal to be determined. Dilatational waves propagate in the bone which could be considered as a biological solid material.The wave propagation mode is in an infinite medium i.e. the dimension of the medium or transverse dimension of the material is higher than the wavelength. In that case, the theory of dynamic elasticity demonstrates that the velocities are related to elastic constants describing the elastic behaviour of the material of interest. Longitudinal, transverse velocities measured are also called bulk velocities. They allowed to assess the elastic constants then by reversing the matrix of elastic constants (Cij), elastic properties could be assessedsuch as Young's

modulus, Shear modulus and Poisson's ration (E_{ij}, G_{ij}, ν_{ij}).

$$\frac{\partial \sigma_{ij}}{\partial x_j} = \rho \frac{\partial^2 u_i}{\partial t^2} \quad i,j = 1,2,3$$
$$\sigma_{ij} = C_{ijk}\varepsilon_{kl} \tag{1}$$

Calibration setup is performed on materials (Copper, Stainless steel, Plexiglass, PVC) with known values of velocities (5010m/s, 5790m/s, 2680m/s). Bone velocities values are within this range of velocities. Impulse waves were generated by a function generator(HP 3312A). Ultrasonic waves produced by the transducers (2.25 MHz, Panametrics) were recorded and analyzed by a numerical scope (Tektronics 2232). Acoustic and elastic properties were assessed in the three directions. Degree of anisotropy of cortical bone was also investigated at the macro level using the TUC technique (Ho Ba Tho et al. 1992, Bensamoun et al. 2004).The TUI technique used the same theory but allowed to provide a cartography mapping of ultrasound velocities (Bensamoun et al. 2004). In fact, the experimental set up is different, samples are in immersion and focused transducers (4MHz) were used. Measurements of longitudinal velocities will bedetermined through an ultrasonic method. A part of the acoustic wave is reflected back to thetransducer acting this time as a receiver, which transformsthe acoustic wave into an electrical pulse in orderto obtain longitudinal acoustic velocities on eachfemoral section. The acoustic transducer is held by acolumn, which is controlled by a microcomputer. Inorder to obtain many measurements on the surface ofthe specimen the transducer is translated with a step of0.5mm with an accuracy of 1 mm on the X-axis. Thedisplacements are driven by a computer which uses acustom made program (Cactus)controlling a micrometer translation stage.The number of points of acquisition varies from 1460to 1734 for the focused transducer. The wave velocity(m/s) is then expressed by the length (m) differencebetween the specimen and the measured time delay (ms):v 1/4 2e=t; e being the average thickness of the crosssection and t the time delay. Finally the computeracquires data and using Cactus, a colour map of the acoustic velocities of thesurface of the specimen is obtained.

Themeasurement of the apparent density of the samples has been determined by the ratio between the weight and the volume of the samples. The measurement of the weight has been performed by the use of an accurate (0.1mg) balance (Sartorius BP61S). The volume has been determined with the metric measurements, which were performed with a micrometer (Mitutoyo, 293, Japan) which accuracy is 0.01mm.

Morphological measurements such as section area, microporosities, pores shape and size are assessed using a microQCT (Skyscan 1072), and using ESEM and in

house software to assess these information (Bensamoun et al. 2004, Basillais et al. 2007).

Microstructural level

At this level, the tissue properties are investigated at the micron resolution mapped across lamellar bone.Nanoindentation (Hysitron Inc., Minneapolis, MN, USA) was performed on the same specimens in order to assess the elastic properties at the microscopic level (osteon lamella, interstitial lamella). The nanoindenter is equipped with a Berkovich diamond tip; the mechanical tests is carryied out with a holding time of 10 sec at maximum force, to allow viscous strain to develop.Three loading-unloading program were conducted.Three indentations were performed on the thick lamella located in the middle of the osteon. The maximal force is 2500μN, which induces a maximal depth of about 400nm. The reduced modulus (Er) is obtained from the load – displacement experimental curve using the robust Sneddon's equation (2) that has been developed for a contact between an axisymmetric rigid indenter and a homogeneous isotropic half space (Pharr et al. 1992):

$$E_r = \frac{\sqrt{\pi}}{2} \times \frac{S}{\sqrt{A}} \tag{2}$$

A is the contact area and S is the stiffness obtained from the slope on the last unloading. The calibration of the tip area has been performed with indents on fused silica.A total of 351 indentations have been performed on 67 white, 17 grey, 39dark osteons.Statistical tests (ANOVA tests) (Statgraphics V5.0, Sigma plus) were performed to compare the difference between elasticity measured at different scale of the cortical bone tissue. In order to localize the osteons lamellae to be tested, a back scattered environmental scanning electron micrographs (XL 30 ESEM Philips) has been produced under high vacuum at 20KV with a magnification of 45. All the surface of the samples have been scanned with an electron beam in order to have a mapping of back scattered electron reflecting the mineralisation constituting the surface (Figure 3) (Bensamoun et al. 2008).

The anisotropy was also investigated using nanoindentation tests with a Nanoindenter XP (MTS System Corp., Oak Ridge, TN). The Nano indenter XP system hasa load and displacement resolution of 50 nN and0.01 nm, respectively. Indentations were performed at constant quasistatic strain rate in the longitudinal direction of the femur diaphysis using the continuous stiffness measurement (CSM) method. In fact, one should know that basic assumptions using nanoindentation technique are considering homogeneous and isotropic material behavior. Formulations for anisotropic are provided (Swadener and Pharr 2001), but isotropy related equations could be used as a first order approximations (Swadener et al. 2001).In our study, nanoindentation experiments are performed by assuming a homogeneous bone ma-

terialand nanoindentation along different directions have been carried out on the specimens.Measurements of reduced elastic modulus (equation 2) were performed with Berkovich indenter in differentaxes of symmetry of the samples(Vanleene 2006, Vanleene et al. 2008).

With conic indenter it was possible to insvestigate the imprints on isotropic (PMMA) and anisotropic materials such as cortical bone. In order to analyze these imprints, AFM images (AFM, Dimension 3100, Bruker, Santa Barbara, CA) were obtained using tapping mode with 50×50 μm and 80×80 μm image size and 512×512 pixels field of view.The elastic return Δz is reflecting the difference in height between imprint under loading case and that of the unloading case.Furthermore FEM was performed in order to visualize the elastic return in different direction of indentation which is assumed to be parallel to the different axes of symmetry of the sample (Figure 2).A model has been created to simulate the nanoindentation with a conical indenter. Onlya part of the sample is modelled (one hundred by one hundred μm) the model is meshedwith the help of 10,095 hexahedrons and 30 wedges, this results in 11,071 nodes. It wascreated using Abaqus/Standard version 6.9.The indenter is controlled in displacement until 3μm, the contact between the indenterand the sample is defined by a penalty method without friction. Boundary conditions are considered symmetrical due to the conical geometry of the indenter and the cylindrical shape reflecting the osteon geometry. Thematerial has an anisotropic elasticity behaviour and assumed to behave as an elasto-perfectly plasticity (σmax=150 MPa). This constitutive model to describethe nanomechanical behavior may be justifiedby thelong recovery time observed for deformation(Tai et al. 2005).Material data of cortical bone used in the simulation have been obtained by ultrasoundtechnique at the tissue level(Brockaert et al. 2009, Brockaert 2010).

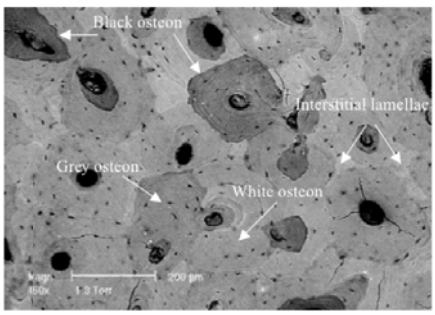

Figure 3: Visualisation of the different osteons (black, grey, white), interstitial lamellae.

2.2.3 At the molecular level (Ultra structure)

At the molecular level, physico-chemical analyses are performed to assess the ratio between matrix and organic components. Fourier Transformed Infra Red (FTIR) spectroscopy analysis was performed on bone samples (1760-X Fourier Transform Infrared Spectrometer, PerkinElmer Inc., Wellesley, MA, USA) (Vanleene 2006, Vanleene et al. 2008). Thespectra were curve-fitted in the ν4 PO4, ν2 CO3 and collagenamide band domains (GalacticGRAMSsoftware, NH, USA).Several parameters were extracted from FTIR datacorresponding to band intensity (band area) ratio of representativespecies relative to all ν4 phosphate domainbands: PO4 species in apatite lattice (sum of 600, 575and 560 cm-1 bands), non-apatitic HPO4 ions located in ahydrated layer on apatite crystal surface (534 cm-1 band),type A CO3, type B CO3 species in apatite lattice (879and 871 cm-1 bands), non apatitic CO3 species (866 cm-1band) and collagen amide I species (1650 cm-1 band).Second, two chemical analyses were performed on samples.Carbonate weight percentage (CO3W%) was measuredusing a CO2 Coulometer(Coulometrics Inc., Co, USA). Protein nitrogen weight contentwas analysed using aElemental Analyser EA 1110 CHNS (Thermo Fisher ScientificInc., MA, USA). Elemental analysis precision is 0.3%.Protein weight percentage of bone (PW%) was then obtainedfrom nitrogen content in collagen. X-raydiffraction was recorded with a X-ray diffractometer (InelCPS 120, Enraf Nonius SA, France) using Co radiation (Xraywavelength =1789A$^{\circ}$). Two peaks at 30?and 45?(2θ) wereidentified respectively to 002 (c-axis of apatite lattice) and310 diffraction planes of the apatite crystals. Nanoscale images of human cortical bone were obtained in air using a commercial AFM (NanoScope III MultiMode AFM, Bruker, Santa Barbara, CA) equipped with a 125 μm $\times$ 125 μm $\times$ 5 μm scanner (J-scanner). Topographic images were recorded in contact mode using oxide-sharpened microfabricated Si_3N_4 cantilevers (Microlevers, Bruker, Santa Barbara, CA) with a spring constant of 0.01 N/m (manufacturer specified), with a minimal applied force ($<$500 pN) and at a scan rate of 2–3 Hz. The curvature radius of silicon nitride tips was $\sim$20 nm. All images shown in this paper are flattened raw data.

All statistical analyses were performed using the softwareStatgraphics Plus Version 5.0 (Statistical Graphics Corp., USA).

2.3 Results

2.4 At the organ level (macroscopic structure)

At this level, it should recalls that tissue properties are investigated across the organ at 100 μm resolution. The range of values of bulk velocities for all femoral sections investigated wasfor the minimum and maximumvalues respectively 3400m/s (dark

blue color) 4400m/s (red color), most frequent values were found around 4000m/s (yellow color) as illustrated in Figure 4 for different levels of the femoral section of F2. Cartographies of bone cortical densities (kg/m^3) are also ranging from 950 to 1900 kg/m^3. Most frequent values were found around 1700 kg/m^3(Figure 5 (b)). The cartography of elastic constant C33 is calculated with the relationship between velocities and densities for each pixel (Figure 5(c)). Range of C33 was in between 15 to 37 GPa (blue, red colors) with frequent values around 25 GPa (yellow color).

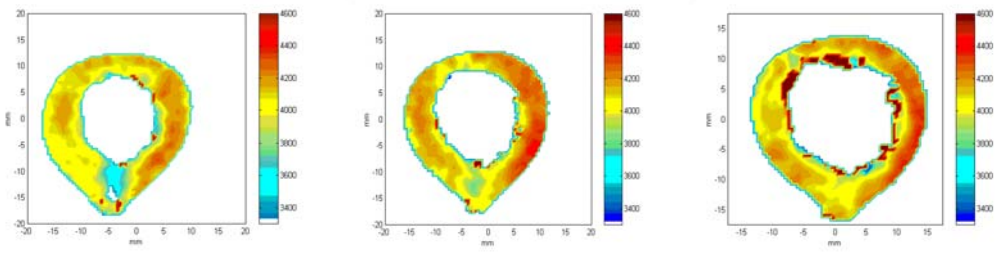

Figure 4: Velocities mapping at 50%, 60% and 70% of the total length of F2.

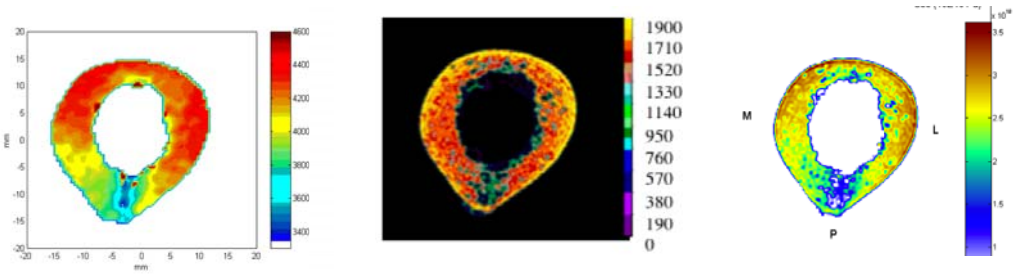

(a) (b) (c)

Figure 5: Cartography of velocities (a), densities (b) and elastic constants C33 (c) of one section (at 40% total length) of F2.

Morphological measurements obtained by micro QCT are illustrated on Figure 6 for the three femurs. Range of values of porosities for the three femurs measured on the cubic samples are summarized in Table 1.

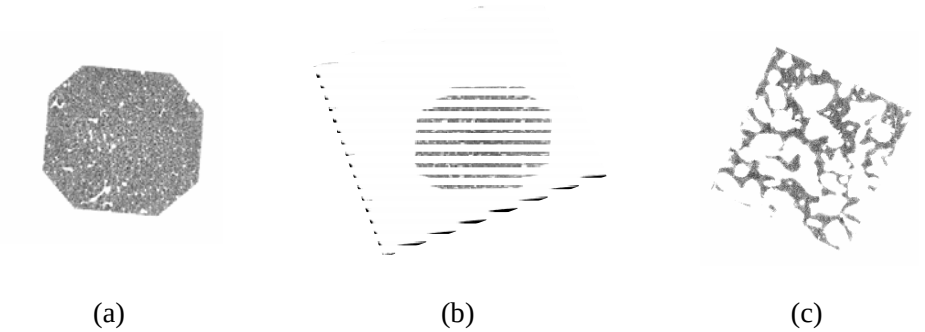

(a) (b) (c)

Figure 6: Variations of morphological properties of the F1 (a), F2 (b), F3 (c) femurs.

Table 1: Values of densities, porosities properties and mean diameter pore size.

	F1 (n=10)	F2 (n=32)	F3 (n=18)
Density (kg/m^3)	1892±30	1650±275	1221±161
min-max	1855-1932	855-2127	979-1688
Porosity (%)	8±3	12±15	59±14
min-max	4-10	3-47	35-72
Mean 'diameter' pore size (μm)	60±13	101±64	404±102
min-max	47-83	47-253	202-610

2.5 At the tissue level (macro-microscopic structure)

At the tissue level (haversian system),the axial Young's moduli (E_cort (macro)) were found to be 21±2, 20±5 GPa, 10±4 GPa for F1, F2, F3 respectively from ultrasound measurements. Tangential Young's moduluswasfound to be13±2 GPa, 12±2 GPa, 7±2 GPa for F1, F2, F3 respectively. Radial Young's modulus wasfound to be12±2 GPa, 11±2 GPa, 6±2 GPa for F1, F2, F3 respectively (Figure 7).

At the microstructural level of the same samples, it should recall that the tissue properties are investigated at the micron resolution mapped across lamellar bone using nanoindentation. Axial elastic modulusof the interstitial lamella (E_IL) was found to be equal to 22±5 GPa, 22±3 GPa, 12±3 GPafor F1, F2 andF3 respectively. Values for Axial elastic modulus of osteon lamellae (E_OL) are also provided (Figure 6).As an example, for F2, Young's modulus measured in the longitu-

dinal direction of the sample, for the white (N=61), grey (N=17) and dark osteons (N=39) were found to be statistically different ($p<0.05$) with respective values of 21.30 ± 3.00 GPa, 19.27 ± 1.78 GPa and 12.95 ± 2.66 GPa (Figure 8).

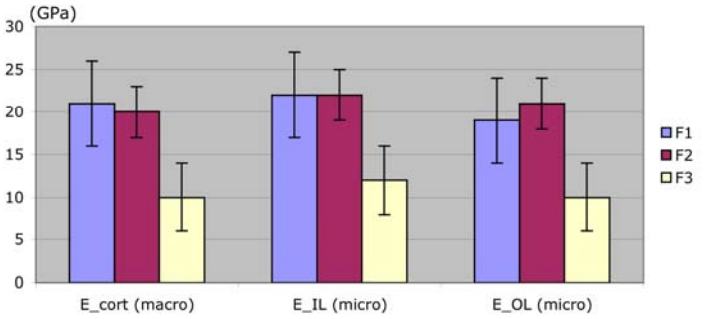

Figure 7: Values of Axial Young's modulus obtained on the haversian system (E_cort (macro)) and on the intersitial lamellae (E_IL), osteon lamellae(E_OL).

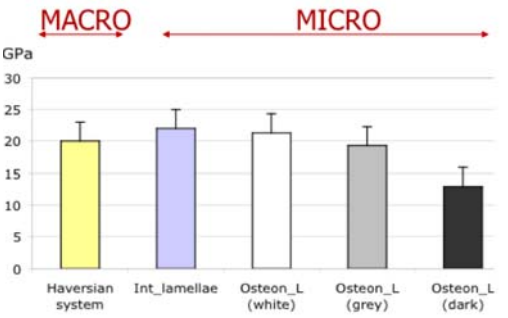

Figure 8: Variations of values of osteon lamellae within samples of F2.

Variation of Young's modulus within the same lamella was investigated by performing three indents on the same lamellae (located approximatively in the middle of the osteon). These results provide quantitative information on the heterogeneity of the single lamellae at the microscale. No significant intralamellae variation ($p<0.05$) was found for the three type of osteons (Table 2). Mean variation of Young's modulus was about 2.72 ± 1.74 GPa with minimum and maximum values of 0.19, 8.48 GPa respectively.

Anisotropy at the microscale has been investigated by performing indentation on the different faces of the sample reflecting the different axes of symmetry of the

Table 2: Variation of Young's modulus values within a lamella for the different type of osteons of F2.

	White osteons	Grey Osteons	Black Osteon
min – max	0.19-7.76	0.93-5.93	0.24-8.48
median	2.81	2.42	2.12
Mean ± STD	2.93-1.83	2.69-1.57	2.45-1.70

sample. Only samples of F2 were investigated.Black and White osteons have been observedon face 1 and 3 of both samples but only whiteosteons on face 2. Young's modulus values werefound higher for interstitial lamellae than for osteonlamellae. Interstitial lamellae values were found higher in longitudinal direction than in transversalones for both samples ($p<0.05$) (Figure 9).

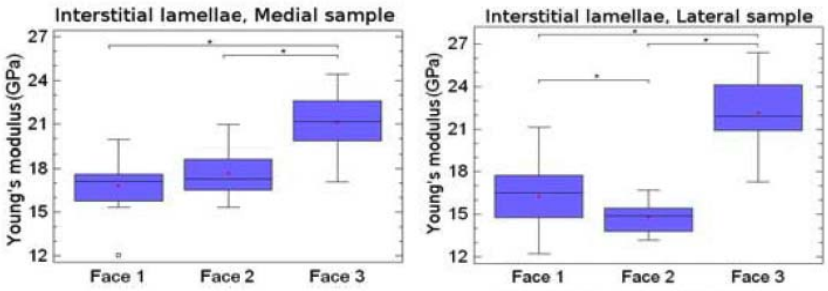

Figure 9: Young's modulus obtained on interstitial lamellae on different faces and samples *(*: significant difference $p<0.05$).*

Young's modulus values were found smaller for black osteons than for white osteons ($p<0.05$). Within osteons, no significant difference was observed ($p>0.05$) (Figure 10).Nanoindentationtest direction seemed to have an influence on Young's modulus values of osteon lamellae but this influence remained weak and non systematic.

Osteon lamellae exhibited astrong heterogeneity of elastic properties accordingto osteon type.

Results of experimental and numerical data concerning the elastic return Δz are illustrated in figure 10. It shows that the isolines of Δz for PMMA are almost circular. For the bone, the shape of the isolines is a special form reflecting bone anistropy.

One would expect a shape of isolines close to a crossshapebut these consistent

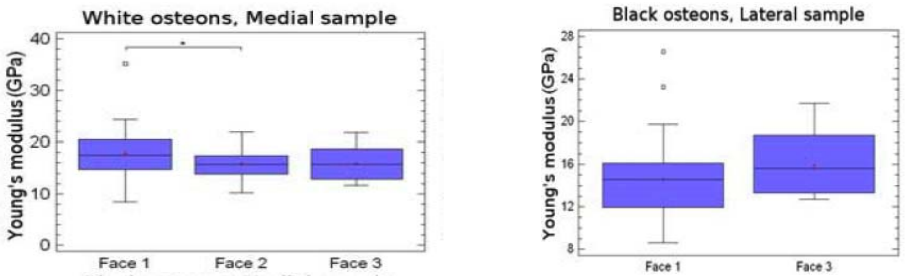

Figure 10: Young's modulus obtained on white and black osteon lamellae on different faces and samples *(*: significant difference $p<0.05$).*

experimental data show the complexity of bone at that scale.The results of FEM show that the evolution of Δz for PMMA is circular at the sample level and for the bone in the longitudinal direction, the shape is elliptical (Figure 11).

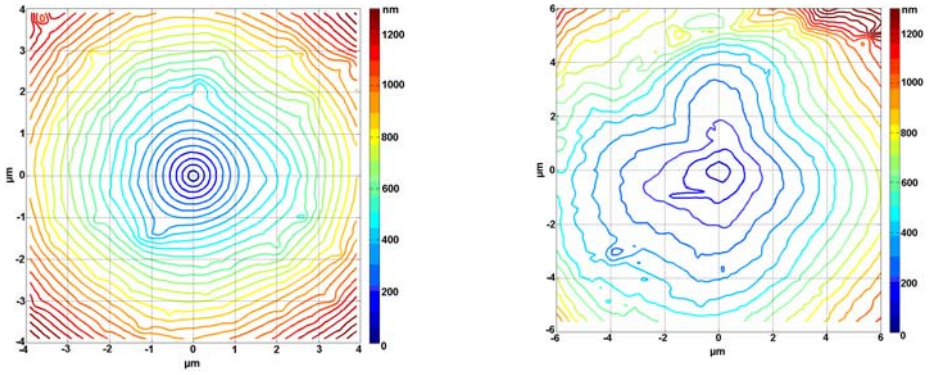

Figure 11: Isolines of experimental Δz for the PMMA (left) and the bone along the longitudinal axis (right)

These results suggest that the anisotropy of the material influence the measurement results. A confrontation with FEM simulation should be necessary to identify the full elastic anisotropic behavior at the microstructural scale.

2.6 At the molecular level (ultrastructure)

FTIR investigations on different femurs are summarized in Table 3. Besides a tendancy of decrease for apatic phosphate and increase for labile phosphate from

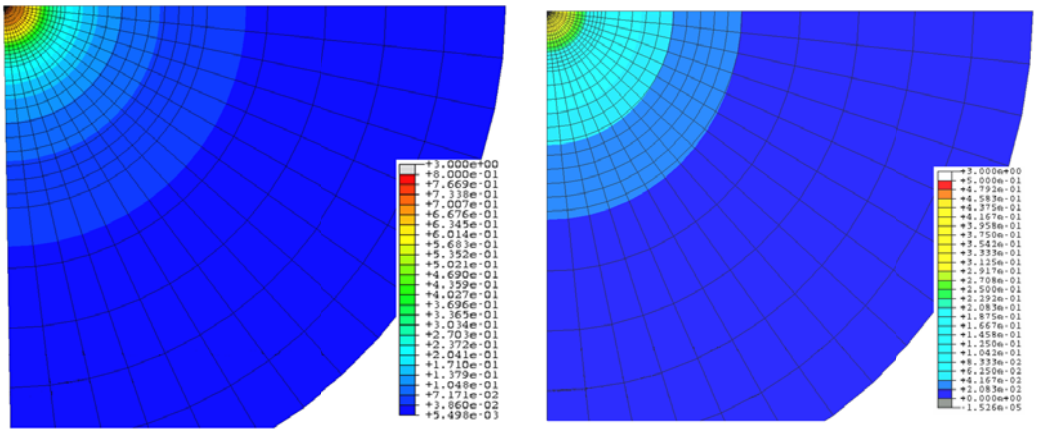

Figure 12: Isolines of numerical Δzfor the PMMA (left) and the bone along the longitudinal axis (right)

F1to F3 (decreasing bone density), no significant difference was found.

Table 3: FTIR band intensity ratio of different componants (mean and standard deviation).

	F1	F2	F3
Apatite PO_4/PO_4	0.68±0.06	0.65±0.08	0.62±0.05
Labile HPO_4/PO_4	0.22±0.04	0.24±0.07	0.27±0.04
TypeA CO_3/PO_4	0.10±0.01	0.12±0.01	0.12±0.02
TypeB CO_3/PO_4	0.31±0.04	0.34±0.04	0.28±0.14
Labile CO_3/PO_4	0.59±0.05	0.52±0.05	0.49±0.04

Same observation is made for analysis of Type A, type B CO_3 and labile CO_3 on total phosphate. Variations of PW% observed confirmed those observed with FTIR analyses. Values for PW% were 42±11, 44±6, 45±5 for F1, F2, F3 respectively.

X Ray diffraction assessments show range of values for the femurs of crystal width about 55 to 110nm and length about 150 to 200nm. These data were confirmed by the visualization of AFM images performed on the femurs (figure 13).

However one should note that some collagen fibers could be observed on F2 and F3 human cortical samples as illustrated on the figure 12 (white arrows).

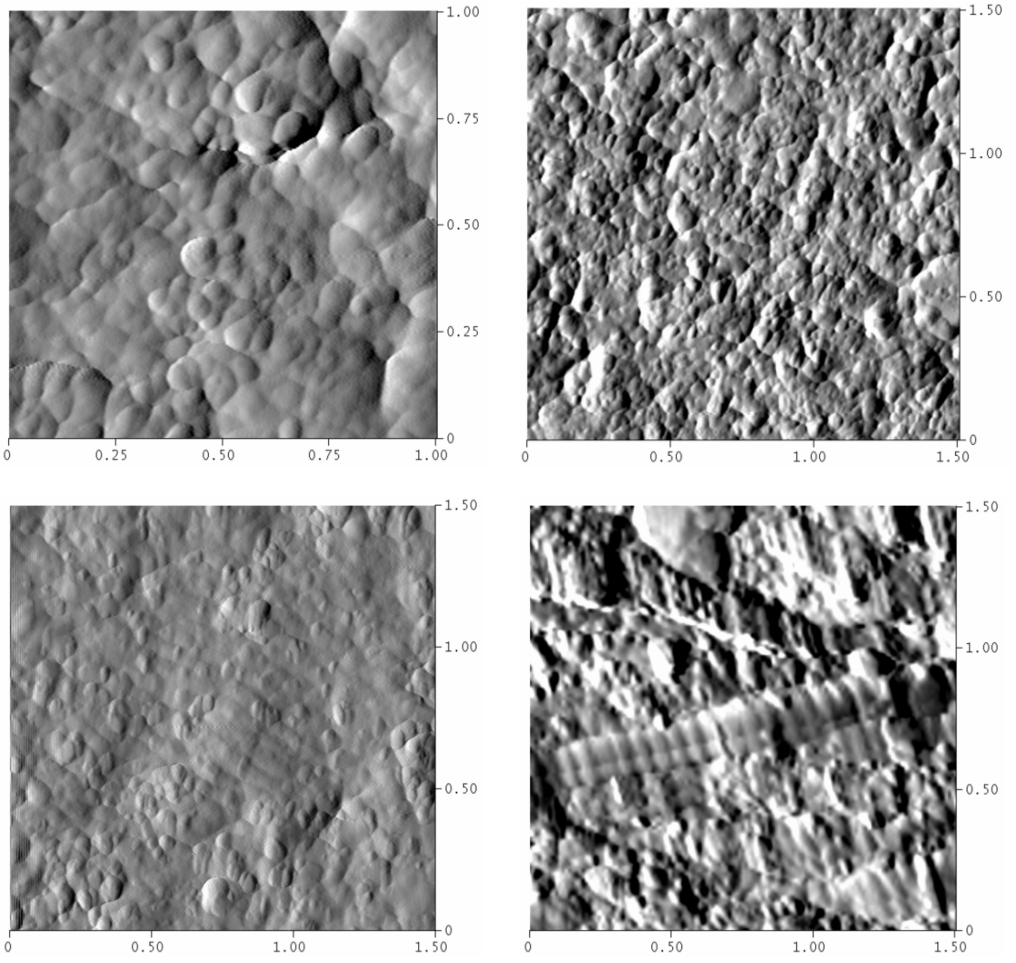

Figure 13: AFM images of femurs F1 (top left and right) and F2 (bottom left) and F3 (bottom right); deflection images scales are in μm.

3 Discussion

At the macroscopic level, values are within the range found in numerous literature data. The different mapping of velocities, densities, elastic properties showed clearly the variation of the mechanical properties according to anatomical variation. One should note that these variations with the same section of the bone has significant variation maximum variation was found to be about 20%, 50% to 70% for velocity, elasticity and density parameters respectively. These results suggest that to detect a variation of 70% of density within the same section a change of 20% of velocity and 50% of elasticity may be expected.

At the microscopic level, values of elastic moduli obtained with interstitial lamellae are slightly lower than that found by previous authors for cortical femoral and tibial bone (about 25-27 GPa). For osteon lamellae elastic properties values are in agreement with that found in the literature. One should note that in the literature, the different degree of mineralization of the osteon are not specified in opposite with our study. In the present study, elastic properties at the microstructural level vary about 40%. This phenomenon reflects the remodelling process at the microstructural level.

The fact that the bone is anisotropic at the macroscopic level implies that nanoindentation on such specimen should be taken with care on the values of Young's modulus obtained. The direction of indentation and face orientation demonstrated its influence on the measurements. Besides it is quite interesting to note that values were consistently different for the three faces only for the instertitial lamellae with highest values for the longitudinal direction of indentation or face 3. It suggests probably that the structural organisation is finished compared to the other osteon lamellae which are in modelling, remodelling process. The experimental and numerical calculation of Δz suggest that the determination of the anisotropic behavior at the microscale of the bone would need investigation such as identification process of the imprints and load curves to assess the full elastic properties.

At the ultrastructural level, no significant difference was found between these three femurs. These results should be confirmed with more data or different models of bone variations or pathologies. As they all represent normal bone, one could expect no significant difference at that scale. Besides ifother samples investigated representing young age (in maturation) or else (pathology) one may expect some significant changes.

Finally, for the present study, microporosities had an important effect on variation of mechanical properties and also on the anisotropic behavior at the macroscopic scale. The mathematical model we developed, allowed to test the influence of the different patterns measured at the microstructural levels and their effect on the

macroscopic anisotropic behavior. The macroscopic values predicted by the variational approaches (Bornert et al. 1996, Ho Ba Tho et al. 2006) are within the range of the experimental values obtained in the present study and also in previous studies (Table 4). It is interesting to notice that in the first assumption of the isotropic behavior of the mechanical properties at the microstructural level, one can predict the anisotropic elastic properties related to structural properties. With the model, we can test the influence of the structural and material anisotropy at the microstructural level on the macroscopic values. These simulations will provide a better understanding of the relationships between structural and material properties at different scale.

Table 4: Values of elastic properties (Shear Modulus, Young's modulus, Poisson's ratio) at the macroscopic level obtained by the mathematical model and the experiment.

	G_{12} (GPa)	G_{23} (GPa)	E_3 (GPa)	ν_{12}
predicted	5.30-6.16	6.032-6.66	17.34-19.57	0.214
Experimental	3.5±0.4	4.5±0.4	20±2	0.35

4 Conclusions

Multiscale experimental characterization is of importance to understand consequences of bone mechanical properties alterations from the molecular level to the organ level. Challenges are to investigate the effect of alteration at the nanoscale on the higher scale, but changes occurring at the nano-microscopic level may not be detected at the macro structural level, unless they are significant. In that purpose mathematical modelling are needed in parallel to provide the threshold of significant alterations of one scale to another scale.This knowledge will allow a better comprehension of bone ageing and pathology and contribute to tools for its evaluation, treatment.

Acknowledgement: This study is supported by the Ministère de l'Education Nationale, de l'Enseignement Supérieur et de la Recherche through the Programme PluriFormation "Nanobiotechnologies" and by the CNRS (Centre National de la Recherche Scientifique) and INSERM (Institut National de la Santé Et de la Recherche Médicale) through a joint program IT2B 'Ingénierie Tissulaire Biomécanique et Biomatériaux'.
The authors thank the support of the EUProgramme (MYSPINE project - n°269909).
The authors thank all collaborators who have shared, still share bone testing at different scale.

References

Aoubiza B.; Crolet J.M.; Meunier A. (1996): On the mechanical characterization of compactbone structure using the homogenization theory. *J. Biomech.* 29, 1539.

Ascenzi A.; Baschieri A.; Benvenuti A. (1990): The bending properties of single osteons. *J.Biomech* .23, 763.

Ashman R.B. (1989): Experimental techniques in *Bone Mechanics* edited by S.C Cowin, CRC Press, Inc, Boca Raton, Florida 75-95.

Basillais A.; Bensamoun S.; Chappard C.; Brunet-Imbault B.; Lemineur G. Ilharreborde B.; Benhamou C.L. (2007): Three dimensional characterization of cortical bone microstructure by micro-computed tomography: validation with ultrasound and microscopic measurements. *J. Orthop. Sci.,* 12, 141-148.

Bensamoun S.; Fan Z.; Ilharreborde B.; Rho J.Y.; Ho Ba Tho M.-C. (2008): Assessment of mechanical properties of human osteon lamellae exhibiting various degrees of mineralization by nanoindentation. *J Musculoskel Res*, 11(3), 135-143.

Bensamoun S.; Ho Ba Tho M.-C.; Gherbezza J.-M.; de Belleval J.-F. (2004): Transmission scanning acoustic imaging of human cortical bone and relation with the microstructure. *Clin Biomech* 19: 6. 639-647.

Bensamoun S.; Ho Ba Tho M.-C.; Luu S.; Gherbezza J.-M.; de Belleval J.-F. (2004): Spatialdistribution of acoustic and elastic properties of human femoral cortical bone. *J Biomech.* 37, 503.

Bornert M.; Stolz C.; Zaoui A. (1996): Morphologically representative pattern-based bounding in elasticity. *J Mech. Phys. Solids.* 44, 307.

Brockaert H.; Mazeran P.E.; Rachik M.;Ho Ba Tho M.-C. (2009): Nanoindentation on isotropic and anisotropic materials confrontation with FEM simulations. *Computer Methods in Biomechanics and Biomedical Engineering* 12, 91-92.

Brockaert H. (2010): Caractérisation du comportement anisotrope de l'os à l'échelle microscopique. PhD dissertation Université de Technologie de Compiègne.

Carnelli D.; Gastaldi D.; Sassi V.; Contro R., Ortiz C.; Vena P. (2010): A finite element model for direction-dependent mechanical response to nanoindentation of cortical bone allowing for anisotropic post-yield behavior of the tissue. *Journal of Biomechanical Engineering*, vol 132, 1-10.

Crolet J.M; Racila M.; Mahraoui R.; Meunier A. (2005): A new numerical concept formodelling hydroxyapatite in human cortical bone. *Comp. Meth and Biom. Eng*. 8, 139.

Fan, Z.; Rho, J. (2002): Effects of viscoelasticity and time-dependent plasticityon nanoindentation measurements of human cortical bone. *J. Biomed. Mater. Res.* 67:

208–214.

Fan Z.; Swadener J.G.;Rho J.Y.; Roy M.E.; Pharr G.M. (2002): Anisotropic properties of human tibial cortical bone as measured by nanoindentation. *J Orthop Res.* 20(4):806-810.

Fan Z.; Rho J.Y.; Swadener J.G. (2004): Three-dimensional finite elementanalysis of the effects of anisotropy on bone mechanical properties measuredby nanoindentation. *J. Mater. Res.,* 19(1):114–123.

Fritsch A.; Hellmich C.; Dormieux L. (2009): Ductile Sliding Between Mineral Crystals Followed by Rupture of Collagen crosslinks: Experimentally Supported Micromechanical Explanation of Bone Strength. *Journal of Theoretical Biology*, 260, 230-252.

Hellmich C.; Barthélémy J.-F.; Dormieux L. (2004): Mineral-collagen interactions in elasticity of bone ultrastructure–a continuum micromechanics approach. *European J. Mech. A–Solids* 23, 783–810.

Hellmich C.; Ulm F.J; Dormieux L. (2004): Can the diverse elastic properties of trabecular andcortical bone be attributed to only a few tissue-independent phase properties and theirinteractions? Arguments from a multiscale approach. *Biomech Model Mechanobiol*. 2, 219.

Ho Ba Tho, M.C. (2003): Bone and joints modelling with individualised geometric and mechanical propertiesderived from medical image, *CMES: Computer Modeling in Engineering and Sciences*, 4(3&4), 489-496.

Ho Ba Tho M.C.; Laugier P. (2009): Ultrasonic characterization of the Bone in Materials and Acoustics Handbook. Eds M. Bruneau et C. Potel, Edition Wiley ISBN 978-1-84821-074-5, 4, 759-791.

Ho Ba Tho, M.C.; Rho, J.Y.; Ashman, R.B. (1992): Atlasof mechanical properties of human cortical and cancellousbone. In : Van der Perre G., Lowet G., Borgwardt A (eds) *Invivo assessment of bone quality by vibration and wavepropagation techniques, Part II,* ACCO, Leuven, pp. 7-38.

Ho Ba Tho, M.C.; Rho, J.Y.; Ashman, R.B. (1998): Anatomical variation of mechanical properties of humancancellous bone in vitro. In : G. Lowet, P. Rüegsegger, H.Weinans and A. Meunier (eds) *Bone Research inBiomechanics, IOS Press*, pp 157-173.

Ho Ba Tho, M.C.; Stolz, C.; Vanleene M., Bensamoun S.; Treutenaere J.M.; Rey C. (2006): Multi-scale Characterization and Modelling of Human Cortical Bone. *In: Mater. Res. Soc. Symp. Proc. 898E, Warrendale, PA, 2006* Edited by: Andrew J. Bushby, Virginia L. Ferguson, Ching-Chang Ko, Michelle L. Oyen.

Ho Ba Tho, M.C.; Treutenaere J.M. (2001) : Influence ofacquisition parame-

ters on QCT measurements derived fromCT. Proceedings XVIIIth Congress of the International Society of Biomechanics, Zurich, 102-103.

Katz J.L. (1981): Composite materials models for cortical bone in *Mechanical Properties of Bone* edited by S.C Cowin (ASME Symp 145, Boulder, CO, 1981) p. 171.

Meunier A.; Katz J.L; Christel P.; Sedel L. (1988): A reflection scanning acoustic microscopefor bone and bone-biomaterials interface studies. J. Orthop. Res. 6, 770.

Pharr, G.M.; Oliver, W.C.; Brotzen, F.R. (1992): On the generality of the relationship among contact stiffness, contact area, and elastic modulus during indentation.*Journal of Materials Research*, 7(3), 613.

Rho, J.Y.; Ho Ba Tho, M.C.; Ashman, R.B. (1995): Relations of mechanical properties to density and CTnumbers in human bone. *Med Eng Phys*, 17, (5), 347-355.

Rho J.Y; Roy M.E; Tsui T.Y; Pharr G.M. (1997): Elastic properties of human cortical andtrabecular lamellar bone measured by nanoindentation. *Biomaterials* 18, 1325.

Rho J.Y; Roy M.E; Tsui T.Y; Pharr G.M. (1999): Elastic properties of microstructuralcomponents of human bone tissue as measured by nanoindentation. *Biomed. Mater. Res.* 45, 48.

Swadener, J.G.; Pharr, G.M. (2001): Indentation of elastically anisotropic half-spaces by cones and parabolae of revolution. *Philosophical Magazine A: Physics of Condensed Matter, Structure, Defects and Mechanical Properties* 81 (2), 447-466.

Swadener, J.G.; Rho, J.-Y.; Pharr, G.M. (2001): Effect of anisotropy on elastic moduli measured by nanoindentation in human tibial cortical bone. *Journal of Biomedical Materials Research* 57 (1), 108-112.

Tai K.; Qi H.J.; Ortiz C. (2005): Effect of mineral content on the nanoindentation properties and nanoscale deformation mechanisms of bovine tibial cortical bone.*Journal of Materials Sciences : Materials in Medecine* 16, 947-959.

Vanleene M. (2006): Caractérisation multi-échelle des propriétés mécaniques de l'os cortical. PhD Dissertation, Université de Technologie de Compiègne.

Vanleene M.; Mazeran P.-E.; Ho Ba Tho M.-C. (2006): Influence of strain rate on the mechanical behaviour of cortical bone interstitial lamellae at the micrometer scale, *J Mater. Research*, 21, 2093-2097.

Vanleene M.; Mazeran P.E; Ho Ba Tho M.-C. (2008): Influence of nanoindentation test directions on elastic properties of humane cortical lamellae, *Journal of Biomechanics*, 41, S74. Proceedings of the 16th ESB congress.

Zysset P.K.; Guo X.E.; Hoffler C.E.; Moore K.E.; Goldstein S.A. (1999): Elastic Modulus and Hardness of Cortical and Trabecular Bone Lamellae Measured by Nanoindentation in the Human Femur. *J. Biomech.* 32, 1005.